

Detection and Segmentation of Mirror-like Surfaces Using Structured Illumination

Rajat Aggarwal Anoop M. Namboodiri

Kohli Center on Intelligent Systems,
International Institute of Information Technology- Hyderabad, India.

{rajat.aggarwal@research., anoop@}iiit.ac.in

ABSTRACT

In computer vision, many active illumination techniques employ Projector-Camera systems to extract useful information from the scenes. Known illumination patterns are projected onto the scene and their deformations in the captured images are then analyzed. We observe that the local frequencies in the captured pattern for the mirror-like surfaces is different from the projected pattern. This property allows us to design a custom Projector-Camera system to segment mirror-like surfaces by analyzing the local frequencies in the captured images. The system projects a sinusoidal pattern and capture the images from projector's point of view. We present segmentation results for the scenes including multiple reflections and inter-reflections from the mirror-like surfaces. The method can further be used in the separation of direct and global components for the mirror-like surfaces by illuminating the non-mirror-like objects separately. We show how our method is also useful for accurate estimation of shape of the non-mirror-like regions in the presence of mirror-like regions in a scene.

CCS Concepts

•Computing methodologies → Computational photography; *Image processing*;

Keywords

Structured Illumination; Mirror-like surfaces, Segmentation, Projector- Camera

1. INTRODUCTION

Structured light systems are widely used in applications such as machine vision, visual inspection, parts alignment, object recognition, estimating material properties, 3D scanners, space time stereos etc. However, capturing reliable information from a very complex scene including wide range of shapes and materials, is a difficult task. One of these complicated surfaces are mirror like surfaces. Mirror like

Permission to make digital or hard copies of all or part of this work for personal or classroom use is granted without fee provided that copies are not made or distributed for profit or commercial advantage and that copies bear this notice and the full citation on the first page. Copyrights for components of this work owned by others than ACM must be honored. Abstracting with credit is permitted. To copy otherwise, or republish, to post on servers or to redistribute to lists, requires prior specific permission and/or a fee. Request permissions from permissions@acm.org.

ICVGIP '16 Guwahati, Assam India

© 2016 ACM. ISBN 978-1-4503-4753-2/16/12...\$15.00

DOI: <http://dx.doi.org/10.1145/3009977.3010020>

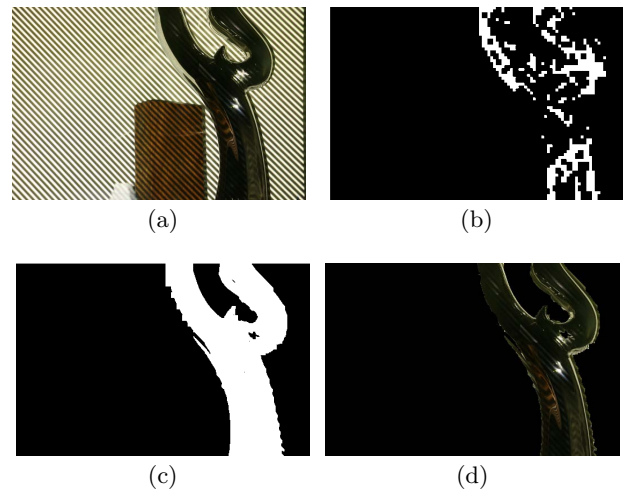


Figure 1: (a)Captured image with sinusoidal pattern projected onto the scene from projector's point of view. (b)Binary image representing the windows which are labelled as the specular regions. (c)Smooth segmentation obtained by applying MRF using Initial segmentation cues (d)Color Image of the specular regions present in the scene.

surfaces are common objects in vision tasks and robot navigation. They are commonly found in indoor environments and its difficult to recognise for a camera whether it is an obstacle or a path. As service robots perform more and more tasks in indoor environments, the ability to recognize mirrors is necessary. In vision, these objects poses a problem for all techniques that are based on feature detection and matching, such as, binocular stereo and Structure from Motion. This is because, the appearance of mirror-like objects depends upon the environment and thus, it is difficult to determine whether an image feature corresponds to an actual scene point or it is the specular reflection of another scene point. The representation of mirror-like surfaces depends not only on the surface properties but also on the properties of the surrounding scene and the viewpoint of the observer. One of the solutions to remove these kind of inaccuracies is to apply separate robust techniques for different surface materials. This makes segmentation of mirror-like surfaces an important problem. Detection of mirror-like surfaces in a scene, can simplify pre-processing steps in many practical tasks in robotic vision algorithms.

In this work, we present an active illumination technique for segmentation of mirror-like surfaces from the scene. We propose a custom setup consisting of a camera, projector and a One-Way mirror which is used to capture the pattern projected onto the scene from the projector’s point of view. It is observed that the captured frequency of the illumination pattern for the specular surfaces, changes when viewed at a distance from projection point. These changes in local frequencies are exploited to segment out the specular regions in the imaged scene. Fig 1a shows the image of the scene captured using our setup from projector’s point of view. Changes in the local frequencies are used to segment the specular regions as shown in Fig 1b. The setup ensures that the change is only due to the nature of the material and not due to the shape and orientation of the objects in the scene.

The major contribution of our work is to provide a custom setup using which we can image the scene from the projector’s point of view. The second contribution of this work is to detect the frequency change in the projected and the observed illumination pattern and use this difference as a cue for segmenting out the mirror like regions. We show experiments on various scenes including mirrors and partially specular objects. We then demonstrate the usefulness of the segmentation to correctly separate out the direct and indirect illumination for the specular objects in a scene. Finally, we point out that this method can be employed to accurately reconstruct the surface if separate robust techniques are applied for different kind of surfaces.

2. RELATED WORK

There has been a lot of work on removing specularity (highlights) from the image as shown in [3] but only a small number of researchers have looked into the issue of detecting specular surfaces and correcting the errors automatically. People have used different sensors to detect mirrors and windows, used the information from the surrounding to detect the feature points and the specular highlights to recognize specular surfaces.

Yang and Wang [26, 27] introduced a sensor fusion technique to detect potential mirror-like obstacles in a 2D occupancy grid map using sonar sensors and a laser scanner. However, their approach works in 2D only. Koch et. al. [11] presented a specular reflectance detection approach applicable to multi-echo laser scanners in order to identify and filter mirrored objects. Agha-mohammadi and Song [2] and Lu et.al. [15] proposed a technique of estimating a mirror transformation matrix and geometric constraints for corresponding real and virtual feature points in the image. However, these approaches assume the presence of feature points from the surroundings as well as their mirror images in the captured scene. Our technique assumes no prior environment information to detect the mirror-like surfaces. Kashammer and nuchter [9] captures a series of 3D laser scans. Laser completely gets reflected when strikes the mirror surface and do not appear in the point cloud at all. However, this is applicable only for framed rectangular mirrors whose dimensions are known.

Other approaches are based on the information from the environment to detect the distortions in a known shape. Oren and Nayar [19] analyze the characteristic and governing geometry of specular surfaces. However, their proposed method is limited to surfaces with high curvature and

does not address detecting and modeling planar specular surfaces. Adato et. al. [1] proposes specular flow, but reconstruct general surface shape under distant, unknown illumination by an environment map and a static observer. In their approach, the relative positions between the camera and the object must remain static, that is, only the environment map is allowed to move. Vasilyev et. al. [24] extends this approach and shows that one specular flow is needed to construct the shape of mirror-like surfaces. Savarese and DalPozo [6] proposed the features called as static specular flow (SSF), which are based on capturing the distortions of the surrounding scene due to the curvatures in the reflecting surface. However, such kind of specular features are only applicable to the curved reflective surfaces in proximity of either occluding contours of the object or regions where the difference of the two surface principal curvatures is high. In practice, objects need not always be curved and have SSF will not detect any distortion. Secondly, this approach is only applicable to the surrounding scenes with textures. Yilmaz *et al.* [28] proposed an algorithm that relies on scale and rotation invariant feature extraction techniques and uses motion cues to detect and localize specular surfaces. Geometry of the object requires to be known a priori in such approach. Osadchy *et al.* [20, 21, 18] uses specular highlights as the cue for segmentation. However, specular highlights are not always detectable and often even completely absent from the object. This is because the perceived brightness becomes a strong function of the viewpoint due to highlights or reflections from the source. Hence they cannot be used as a main or unique cue for recognizing specular surfaces. To reduce these kind of ambiguities in the specular highlights, we propose to capture the specular reflections from the source’s point of view. The main goal of our work is to provide an approach which only depends on the surfaces which are present in the scene.

Our goal is to come up with an active illumination technique which can be used to detect the specular surfaces without any prior information about the surrounding environment. Active illumination is also being used for image segmentation as shown in the work by Raskar et. al [22] who strategically positioned flashes to produce an edge depth map computed from a series of images, whereas koh et. al [12] uses multi-coloured lamps are used in place of the flashes which allows simultaneous acquisition of the images. Active lighting is also used in assisting the detection of specular surfaces. For example, Reiner and Donnaer [10] utilize stereo vision and a two dimensional array of light sources for constructing specular surfaces. Kutulakos and Steger [14] introduce a light-path triangulation method for constructing refractive and specular 3D objects, in which the light source must move along the light ray while the camera captures two consecutive images of the reflected light. Other active illumination methods are reconstruction methods [7, 25, 4] use a continuous area illumination or a single display to cast coded patterns onto the mirror-like object and use a multi-view approach to resolve the surface shape. Tin et. al. [23] proposes efficient ray coding scheme to reconstruct mirror type surfaces. Nayar and Gupta [16] proposes diffuse structured light by placing a diffuser between the light source and the scene. Their approach helps in reducing both specularities and shadows in structured light methods. These active illumination methods reconstructs the surface, when the scene contains specular objects and can not be used for

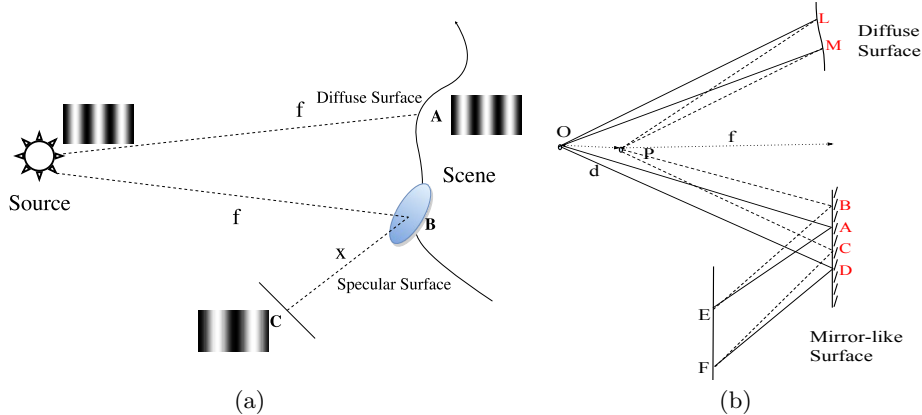


Figure 2: (a,b)Pattern projected on the specular surface is reflected from point C which is not necessarily in the scene. This changes the frequency of the pattern observed at a distance d from the projector's point of view P .

discriminating between specular and non-specular regions in a scene. Whereas our method does not have any prior information about the presence of specular surface. Comparison of different approaches for detection/segmentation of mirror-like surfaces, on the basis of the assumptions and Pros/Cons of each approach is shown in Table 1.

	Method	Assumptions	Pros/Cons
[27, 11, 2]	Sensors or Laser Scan	Only Mirrors	Bulky and Expensive
[15, 9]	Geometric Transformations	Only Mirrors; known mirror dimensions	Both world points and its mirror image is captured
[6]	Specular Flow	Curved Surfaces; Textured Environment	mirror-like surfaces, single natural image
Ours	Structured Illumination	known frequency value	mirror-like; single image

Table 1: Comparison of different approaches for detection/segmentation of mirror-like surfaces, on the basis of the assumptions and Pros/Cons of each approach.

3. ILLUMINATING MIRROR-LIKE SURFACES

Consider a scene illuminated by a projector which projects a pattern with known local frequency as shown in Fig 2a. Distance between the projector and the scene is equal to the focus f of the projector. Let us consider a perfectly reflecting surface B in the scene. Any ray coming from the projector is reflected and projected to some other surface point C in the world. C might be inside or outside the imaged scene. The rays are now projected at $f + x$ distance where x is the distance between the surface of the mirror and C . When the scene is viewed from projector's point of view, reflected rays traces same path from C and the observed frequency of the reflected pattern is same as the projected pattern.

As shown in Fig 2b, a pattern of angular frequency ω_p is projected from point P , such that regions BC and LM are

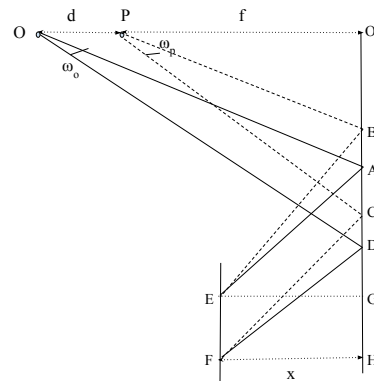


Figure 3: Derivation of the relation between the observed frequency and the projected frequency for the mirror-like surfaces.

illuminated by one complete frequency cycle. Rays from the mirror-like surface reflects at world points E and F which are outside the scene. When this scene is viewed from P , the rays trace the same path and the observed angular frequency for mirror-like surfaces remains same. Since, there is no reflection on diffuse surfaces, the observed angular frequency for diffuse surfaces is also unchanged. It is to be noted that the points in red represents the spatial locations in the image plane, such that the length LM represents the number of pixels(N) spanned by one frequency cycle for which the angular frequency is calculated by $2\pi/N$.

When the observation is taken from point O , which is linearly shifted by distance d from P , the length spanned by one complete frequency cycle remains LM for a diffuse surface, whereas for a mirror-like surface, the length spanned is AD as shown in the Fig 2b. This is because, the sinusoidal pattern which is projected at EF , now traces back the path through AD to reach at the observation point O . Consider a sinusoidal frequency pattern which is projected from point P at an angular frequency of ω_p , such that, one cycle of the frequency pattern is projected at BC as shown in Fig 3. Mirror-like surface reflects the rays at EF and the observed angular frequency at O be ω_o . Let $\angle O'PB = \theta_1$

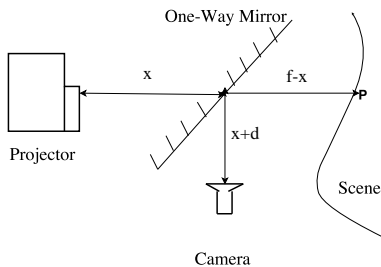


Figure 4: Camera-projector alignment for capturing images from projector's point of view using One-way mirror. Rays pass through the One-way mirror and gets reflected back from point P in the direction of the camera. Camera is at distance d and captures the image from projector's point of view.

and $\angle O'OA = \theta_2$, such that

$$\frac{O'B}{f} = \tan \theta_1, \frac{O'B + BC}{f} = \tan (\theta_1 + \omega_p) \quad (1)$$

From observation point O , we get

$$\frac{O'B + BA}{f + d} = \tan \theta_2, \frac{O'B + BA + AD}{f + d} = \tan (\theta_2 + \omega_o) \quad (2)$$

Also, from $\triangle AEG$ and $\triangle BEG$, $AB = x(\tan \theta_1 - \tan \theta_2)$, from $\triangle CFH$ and $\triangle DFH$, $CD = x(\tan (\theta_1 + \omega_p) - \tan (\theta_2 + \omega_o))$. Solving these equations we get,

$$\omega_o = \arctan \left(\tan \omega_p \left(\frac{f + x}{d + f + x} \right) \right) \quad (3)$$

As d increases, ω_o decreases and $CD > BA$. From Fig 3, $AD = AC + CD$ and $BC = BA + AC$, which implies $AD > BC$. Therefore, when an illumination pattern with known local frequency is projected onto the scene and image is the captured at a distance from projector's imaging plane, the observed local frequency of the projected pattern is changed. Whereas for non-mirror-like regions, captured frequency remains equal to the projected frequency ideally. It must be noted that the frequency change is primarily due to change of depth, when observing mirror like surface because it focus at some other point in the world. Also, the analysis holds for both flat and curved surfaces given that the projector and camera are coaxial. In next section, we show the custom projector-camera setup to capture the image from observation point O .

3.1 System Setup and Illumination Pattern

To implement the mentioned approach, we designed a Projector-Camera setup as shown in Fig 4, which is used to capture the image from the projector's point of view. To achieve this, we use a 'One-Way Mirror' (A one-way mirror has a reflective coating applied in a very thin and sparse layer. It is also called as half-silvered surface) in between the projector and the scene such that all the rays projecting from the projector passes through the one-way mirror and then illuminates the scene. We use this property to capture the image from exact projector's point of view by keeping the camera perpendicular to the projector's direction. Any ray coming from the projector hits the object present in the

scene and is reflected back in the one-way mirror by tracing the exact same path.

In case when one side of the one-way mirror is brightly lit and the other is dark, it allows viewing from the dark side but not vice versa. Thus, the camera only captures the scene which is in front of the one-way mirror and not the other side of the mirror. In order to capture the image from point O , camera is placed at a distance $x + d$ from One-way mirror. All the projected rays trace back at the same focus point when $d = 0$ and camera behaves as if looking from projector's point of view P . Height of the camera and the projector should be same. The benefit of such a setup is that we are restricted to one single and fixed viewpoint and the analysis of our algorithm is done using one single viewpoint. Otherwise for the mirror-like surfaces, the reflections and the perceived image is a function of viewpoint and the environment illumination. Also, the setup ensures that the change is only due to the nature of the material and not due to the shape and orientation of the objects in the scene.

4. SEGMENTATION BY ILLUMINATION

4.1 Local Frequency Analysis

In the proposed setup consisting of a perspective camera and a perspective projector, which projects a sinusoidal pattern onto the scene. We used the pattern $f(x, y) = \frac{h}{2}[1 + \cos(\omega_1 x + \omega_2 y)]$, where ω_1 and ω_2 are the angular frequencies on the sinusoids in radians per pixel, and h is the amplitude of the pattern.

Fig 1a shows the captured image of the scene illuminated by a sinusoidal pattern. Consider an image captured from the proposed setup. As already discussed, regions where the local frequencies are increased or decreased by some amount in comparison to the actual projected frequencies of the pattern gives a simple cue to the mirror-like surfaces. To find the cues for such regions we apply Short Time Fourier Transform on the whole image. We take small windows of size w slided by size s . For each response in the sliding window, we firstly suppress the DC component of the response and find the frequency peaks in the response. Since the actual projected frequency is known, for the windows which have the response is equal to the actual frequency is labelled as the non-mirror-like windows as shown in Fig 1b. These cues are used as the initial segmentation for the mirror-like regions. However, the second maximum peak after the DC component is suppressed will be for the actual pattern projected. If it is not the case then the maximum frequency will be for some other pattern which might be due to the texture of the object or the some other inter reflections. Inter-reflections are discussed in detail in next section.

4.2 MRF for surface segmentation

We use Markov Random Field (MRF) approach to accurately find the mirror-like boundaries for better segmentation results as shown in Fig 1c. Image is considered as a rectangular grid of pixels and MRF is created by computing an energy function consisting of data term E_d and smoothness term E_s , such as $E(u) = E_d(u) + E_s(u)$ where

$$E_d(u) = - \sum_i \log p(u_i | z_i)$$

$$E_s(u) = \sum_{i,j \in N} \exp(-||z_i - z_j||^2)$$

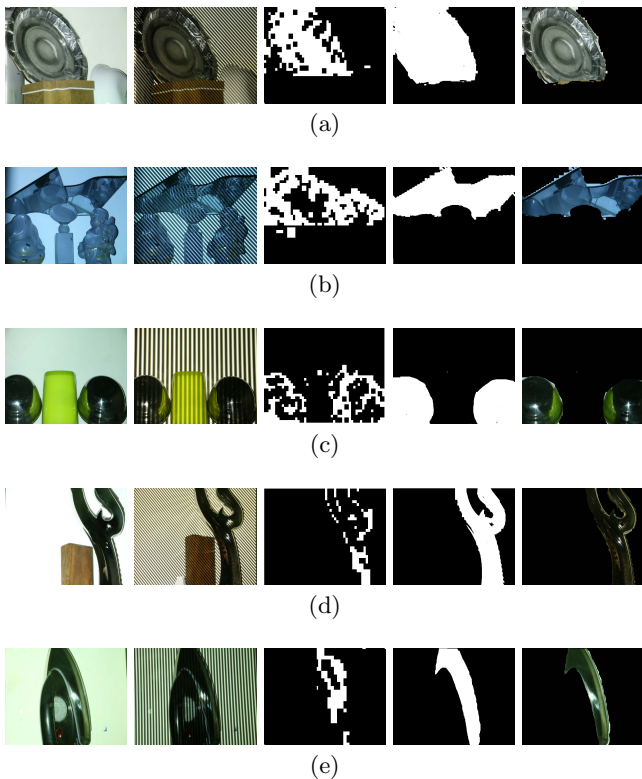


Figure 5: Segmentation Results for various kind of scenes. First column shows the actual image of the scene. Second column shows the image captured with sinusoidal pattern projected onto the scene from projector’s point of view. Third column shows the Binary image representing the windows of size s which are labelled as the mirror-like regions. Fourth column shows the smooth segmentation obtained by applying MRF using Initial segmentation cues. Fifth column shows the colored segmentation result.

where z_i is the pixel color at pixel location i . By analysing the short time frequencies over the captured image, we get a prior knowledge of the mirror-like regions and the non-mirror-like regions. These cues are then used as seeds for segmenting the image by minimizing $E(u)$. This seed is then used for initializing K components of Gaussian Mixture Model (GMM) for both of the regions separately. We first divide both regions into K pixel clusters. The Gaussian components are then initialized from the colors in each cluster. Each pixel is assigned to the GMM component which has the highest likelihood of producing the pixel’s color. A graph is built using the negative log likelihood is the Energy data term for the MRF. Smoothness term is taken as the Euclidean distance between the neighbouring pixels which increase coherence in the energy between similar gray levels. Minimisation is done using a standard minimum cut algorithm in [13] and [5]. This finds a new tentative non-mirror-like and mirror-like regions classification of pixels. These steps are repeated until the classification converges.

5. EXPERIMENTAL RESULTS

In all the experiments, the scene was lit by a NEC digital projector (with 1024x768 pixels) and images were captured using a Canon EOS 70D camera. In practical, observed pattern, $w_{observed}$ is always different from the projected pattern,

$w_{projected}$ due to the differences in resolution of the projector and the camera such as $w_{observed} = k \cdot w_{projected}$. k can be easily found by projecting a light onto plain sheet of paper. Frequency is calculated by locating the cycle of the sinusoidal pattern and the calculating the no of pixels N spanned by that cycle. The frequency then will be $\frac{2\pi}{N}$. Also in practice, One-Way mirror used in the setup produces reflection of the scene onto the other side of the camera. We use a flat mirror behind one-way mirror to completely reflect the reflections. Experimental setup is shown in Fig 12b. Also, it is to be noted that the image captured is inverted from what we see from projector’s point of view. This is because camera is viewing the reflections from the one-way mirror which inverts the image of the scene.



Figure 6: Segmentation result for a scene which includes multiple reflections from one mirror-like surface to another. It also includes the surface which is reflecting the pattern inside the scene.

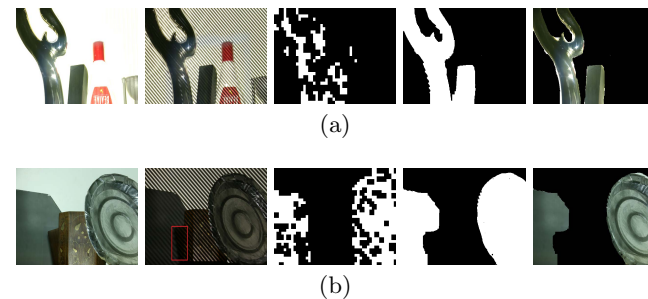


Figure 7: Segmentation results where our approach fails. (a) Black case is dark in color, and hence frequency change can be seen. (b) The distance where the rays are reflected from the mirror-like object (red marked region) is very small. The local frequencies in this region is same as the projected frequencies.

Figure 5 show segmentation results for several scenes where scene is illuminated by a sinusoidal frequency pattern. It can be seen that the mirror-like regions have different frequency as compared to other parts of the scene, and correctly segmented out as shown in Column 4 and 5. Fig 6 shows segmentation results in a scene which have various inter-reflections and multi-reflections. Two mirrors reflect onto each other. As a result, the local frequency in the region is equal to the local frequency observed from the last reflection. Also, the result show the segmentation of the mirror-like surface which is reflecting the pattern inside the scene itself. Since we have projected different frequencies in both directions, our method accurately segments the mirror-like regions even it has frequencies in the inverted directions. Fig 7 shows scenes where our method fails. Fig 7(a) shows scene with a specular idol and a black case. Frequency pattern observed at black case is dark and shows change in frequency, whereas the method works for mirror-like idol. In the region of the mirror-like object as shown in the inset, distance where the mirror-like objects reflects light is almost negligible and there is no change in the local frequencies. As a result, the local frequencies are same as the projected frequency. We found the quantitative results for



Figure 8: (a-c) show the captured images with different frequency pattern. (d) R,G,B boundaries shows the segmentation result by a,b,c patterns, overlaid on the complete image.



Figure 9: (a-d) show the images captured at different camera distances. As the distance d , between the observation and projection point increases, observed frequency on the mirror-like regions decreases.

the segmentation approach by labelling the ground truth images as mirror-like and non-mirror-like regions. ROC curve has been shown in Fig 12a. Average recall and precision rate for the segmentation of mirror-like surfaces is 97.64% and 93.50% respectively. We have experimented with different frequency patterns at different orientations, as shown in Fig 8. Fig 8d shows the segmentation results from three frequency patterns, shown with red, blue and green boundaries. It is observed that the segmentation results do not change much if the frequency pattern changes. Average Recall and Precision values for different frequency is reported in Fig 11b. However, for one frequency pattern, window size taken for computing STFT to calculate local frequency changes the accuracy, as reported in average Recall and Precision value graph Fig 11a. The accuracy is maximum for window size $s = 50$. This shows that the maximum accuracy is obtained at one particular window size. Fig 9 shows the image captured at different relative distances between the camera and the projector. At 9a relative distance is zero and the observed frequency is equal to the pattern frequency. From 9a to 9d, the relative distance is increased. It can be clearly noticed that the captured frequency for the mirror region decreases, whereas, for all other diffuse region, it remains same.

Fig 10 shows the qualitative comparison between our method and the segmentation method proposed by DelPozo and Savarese [6] bases on Static Specular Flow (SSF). SSF is based on capturing the distortions of the surrounding scene due to the curvatures in the reflecting surface. But this method does not segment the regions which are flat and does not capture distortions as shown in Fig 10c. The regions which are not reflecting distortions of the surrounding scene due to the plain scene are not segmented as the mirror-like regions.

5.1 Separation of direct and indirect illumination components

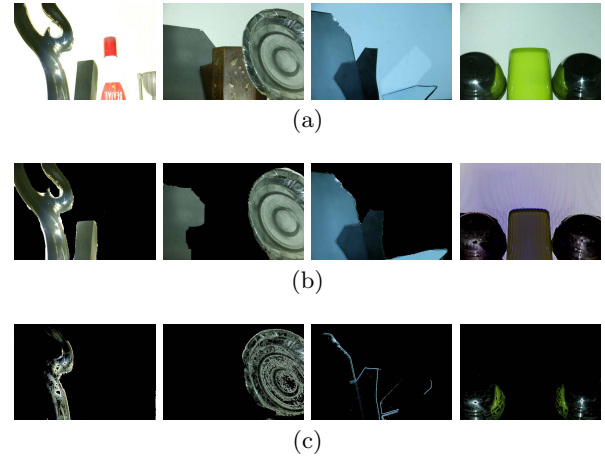


Figure 10: (a) shows the images of the scenes containing mirror-like surfaces. (b) shows the segmentation results from the proposed active illumination method. (c) shows the segmentation results by the method proposed in [6].

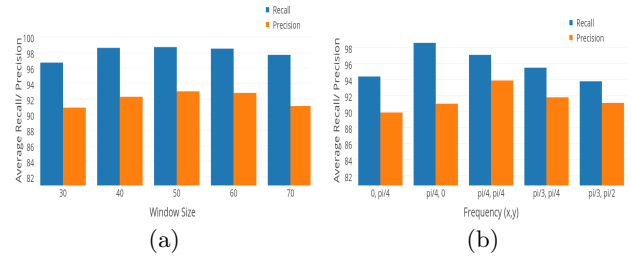


Figure 11: Average Recall/ Precision graph for (a) different window sizes used in STFT. (b) different frequency of the projected pattern.

The behaviour of the specular reflection often leads to problems in many computer vision applications such as stereo matching, segmentation, and recognition. For accurate results, we often separate the direct and indirect components and use one of them in various computer vision applications. Direct illumination is often required as the component for albedo reconstruction. One of the most novel separation methods is shown by Nayar *et al.* [17]. But this technique suffers from the limitations of the direct component of the specular regions which produces errors in reconstruction results. Removing these kind of illumination from the specular regions will correct the direct components for the specular regions which is useful in reconstructing the 3D surface using Shape from Shading methods.

Consider the scene consisting of specular surfaces in it. Direct component is the illumination which is supposed to be reflected directly from the surface and no other part in the world should contribute to that illumination. When a pixel region belonging to a specular surface is illuminated, then the some other pixel region in the world in the direction of reflected ray is also illuminated. In return the world pixel contributes to some of the direct illumination even the world pixel is not illuminated. It is illustrated in Fig 13b, the direct

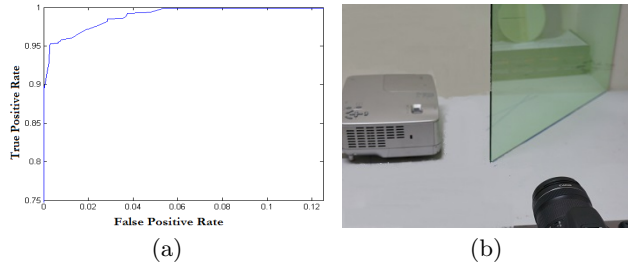


Figure 12: (a)ROC curve illustrating the performance of the approach for segmentation of mirror-like objects in a scene. (b) Image of the experimental setup used in this work.

component for the specular regions contains reflections from the non-specular glass.

We use our setup to illuminate the non-specular regions present in the scene which illuminates the specular surface also. This illumination is the extra component present in the direct component L_d calculated by method in [17]. After we segment out the specular regions from the non-specular regions, we project white light back onto the non-specular regions in the scene for calculating the correct direct components only for the specular regions. We first project three phase shifted sinusoidal pattern and calculate the direct and global component by the method proposed by Nayar *et al.* [17]. We then correct the direct component for specular regions by $L'_{ds} = L_{ds} - I_s$ where I_s is the image pixels in the specular regions when only non-specular regions are illuminated, L_{ds} and L'_{ds} are the initial and corrected direct components for specular regions. It is to be noted that this only corrects the global illumination due to non-specular regions but not from any other specular surface. Fig 13c shows the illumination on the specular regions when only non-specular pixels are illuminated. This gives the extra component I_s which is subtracted from the direct component to give correct direct component which is shown in Fig 13d.

5.2 3D Reconstruction

Estimating the 3D shape of physical objects is one of most useful functions of vision. Texture, shading, contour, stereoscopy, motion parallax and active projection of structured lighting are the most frequently studied cues for recovering 3D shape. These cues, however, are often inadequate for recovering the shape of shiny reflective objects since it is not possible to observe their surfaces directly, rather only what they reflect. This has been illustrated in Fig 14c. In the presence of specular surfaces, light rays are reflected onto the surfaces and the frequencies are changed due to these inter reflections. Such kind of active illumination patterns causes distortions in the actual shape of the idols shown in the figure.

To demonstrate the usability of the problem we separate out the specular regions and reconstruct the remaining lambertian surface using the above technique. We use three phase shift technique in [8] and [30] for 3D reconstruction of the lambertian surfaces. It relies on using three 120-degrees out-of-phase sine waves to determine the column. Given three amplitude values at a given point, we compute the overall phase by looking at the order of the three values by propagating across the 2π discontinuities. This

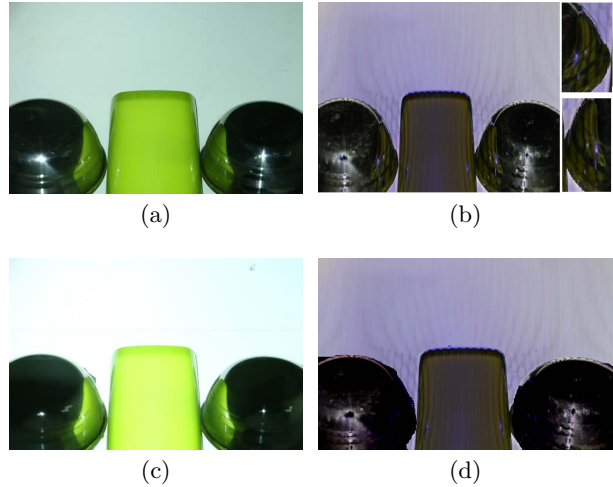


Figure 13: (a) Image obtained by complete illumination of the scene. (b) Direct Component of the illumination obtained from Nayar *et al.* [17]. Inset images shows the reflections from the other objects in the scene in the direct component. (c) Image obtained after illuminating the non-specular regions only. (d) Direct component obtained after subtracting the non-specular illumination component.

phase map can be converted to the depth map by a phase to height conversion algorithm based on triangulation. A simple phase-to-height conversion algorithm is described in [29]. Fig 14d shows the shape reconstruction results by illuminating the non-specular regions only. Under such illumination, there are no inter-reflections due to the specular surfaces and hence no extra distortions in the shape. Comparison between the before and after results are shown in Fig 14d.

6. CONCLUSION

In this paper, we have proposed an active illumination technique for segmentation of specular surfaces by imaging a scene using sinusoidal frequency pattern. The proposed approach requires no prior information about the geometry or textures about the surrounding environment. Segmentation results in the scenes with multiple reflections and inter-reflections are shown. This work shows the usefulness of segmentation of specular surfaces in separating direct component for specular regions accurately. In the end, we point out the application of the segmentation approach in accurately recovering the 3D shape of the surfaces in presence of complex scenes.

7. REFERENCES

- [1] Y. Adato, Y. Vasilyev, O. Ben-Shahar, and T. Zickler. Toward a theory of shape from specular flow. In *Computer Vision, International Conference on*, 2007.
- [2] A.-a. Agha-mohammadi and D. Song. Robust recognition of planar mirrored walls using a single view. In *Robotics and Automation, International Conference on*, 2011.
- [3] A. Artusi, F. Banterle, and D. Chetverikov. A survey of specular removal methods. In *Computer Graphics Forum*, 2011.

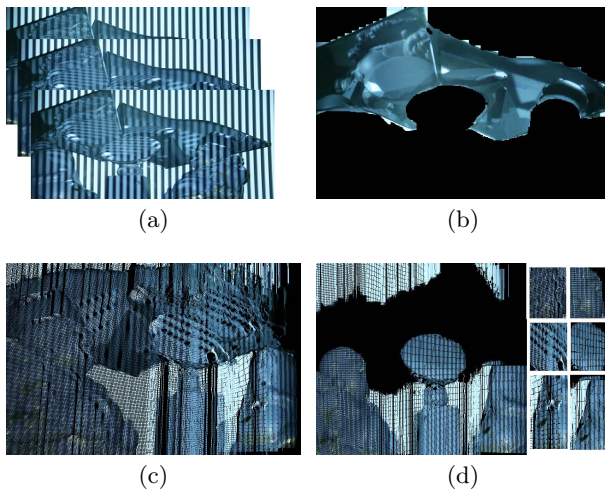


Figure 14: (a) Sequence of images obtained at phases $-2\pi/3$, 0 and $2\pi/3$. (b) Segmented specular regions (b) Shape reconstruction using three phase shift method. The surface has errors in the regions where specular surface reflects light and causes change in the frequencies. (d) Correct shape reconstruction result obtained after projecting patterns on non-specular regions. In the inset, comparison between the before and after separation results are shown.

- [4] J. Balzer, D. Acevedo-Feliz, S. Soatto, S. Höfer, M. Hadwiger, and J. Beyerer. Cavletometry: Towards holistic reconstruction of large mirror objects. In *3D Vision, International Conference on*, 2014.
- [5] Y. Y. Boykov and M.-P. Jolly. Interactive graph cuts for optimal boundary & region segmentation of objects in nd images. In *Computer Vision, International Conference on*, 2001.
- [6] A. DelPoza and S. Savarese. Detecting specular surfaces on natural images. In *Computer Vision and Pattern Recognition, IEEE Conference on*, 2007.
- [7] Y. Francken, T. Cuypers, T. Mertens, J. Gielis, and P. Bekaert. High quality mesostructure acquisition using specularities. In *Computer Vision and Pattern Recognition, IEEE Conference on*, 2008.
- [8] P. S. Huang and S. Zhang. Fast three-step phase-shifting algorithm. *Applied optics*, 2006.
- [9] P. Käshammer and A. Nüchter. Mirror identification and correction of 3d point clouds. *The International Archives of Photogrammetry, Remote Sensing and Spatial Information Sciences*, 2015.
- [10] R. Kickingreder and K. Donner. Stereo vision on specular surfaces. In *Proceedings of IASTED conference on visualization, imaging, and image processing*, 2004.
- [11] R. Koch, S. May, P. Koch, M. Kühn, and A. Nüchter. Detection of specular reflections in range measurements for faultless robotic slam. In *Robot 2015: Second Iberian Robotics Conference*, 2016.
- [12] T. K. Koh, N. Miles, S. Morga, and B. Hayes-Gill. Image segmentation using multi-coloured active illumination. *Journal of Multimedia*, 2007.
- [13] V. Kolmogorov and R. Zabih. Multi-camera scene reconstruction via graph cuts. In *Computer Vision, European Conference on*. 2002.
- [14] K. N. Kutulakos and E. Steger. A theory of refractive and specular 3d shape by light-path triangulation. *International Journal of Computer Vision*, 2008.
- [15] Y. Lu, D. Song, H. Li, and J. Liu. Automatic recognition of spurious surface in building exterior survey. In *International Conference on Automation Science and Engineering (CASE)*, 2013.
- [16] S. K. Nayar and M. Gupta. Diffuse structured light. In *Computational Photography, International Conference on*, 2012.
- [17] S. K. Nayar, G. Krishnan, M. D. Grossberg, and R. Raskar. Fast separation of direct and global components of a scene using high frequency illumination. *ACM Transactions on Graphics (TOG)*, 2006.
- [18] A. Netz and M. Osadchy. Recognition using specular highlights. *IEEE transactions on pattern analysis and machine intelligence*, 2013.
- [19] M. Oren and S. K. Nayar. A theory of specular surface geometry. *International Journal of Computer Vision*, 1997.
- [20] M. Osadchy, D. Jacobs, and R. Ramamoorthi. Using specularities for recognition. In *Computer Vision, International Conference on*, 2003.
- [21] M. Osadchy, D. Jacobs, R. Ramamoorthi, and D. Tucker. Using specularities in comparing 3d models and 2d images. *Computer Vision and Image Understanding*, 2008.
- [22] R. Raskar, K.-H. Tan, R. Feris, J. Yu, and M. Turk. Non-photorealistic camera: depth edge detection and stylized rendering using multi-flash imaging. In *ACM transactions on graphics (TOG)*, 2004.
- [23] S.-K. Tin, J. Ye, M. Nezamabadi, and C. Chen. 3d reconstruction of mirror-type objects using efficient ray coding. 2016.
- [24] Y. Vasilyev, T. Zickler, S. Gortler, and O. Ben-Shahar. Shape from specular flow: Is one flow enough? In *Computer Vision and Pattern Recognition, IEEE Conference on*, 2011.
- [25] M. Weinmann, A. Osep, R. Ruiters, and R. Klein. Multi-view normal field integration for 3d reconstruction of mirroring objects. In *Computer Vision, International conference on*, 2013.
- [26] S.-W. Yang and C.-C. Wang. Dealing with laser scanner failure: Mirrors and windows. In *Robotics and Automation, International Conference on*, 2008.
- [27] S.-W. Yang and C.-C. Wang. On solving mirror reflection in lidar sensing. *IEEE/ASME Transactions on Mechatronics*, 2011.
- [28] O. Yilmaz and K. Doerschner. Detection and localization of specular surfaces using image motion cues. *Machine vision and applications*, 2014.
- [29] C. Zhang, P. S. Huang, and F.-P. Chiang. Microscopic phase-shifting profilometry based on digital micromirror device technology. *Applied optics*, 2002.
- [30] S. Zhang and P. Huang. High-resolution, real-time 3d shape acquisition. In *Computer Vision and Pattern Recognition Workshop, IEEE Conference on*, 2004.